ACS OMEGA

Open Access

http://pubs.acs.org/journal/acsodf

Article

Charging and Discharging of Poly(*m*-aminophenylboronic Acid) Doped with Phytic Acid for Enzyme-Free Real-Time Monitoring of Human Sweat Lactate

Ryujiro Kishi, Shoichi Nishitani, Hiroyuki Kudo, and Toshiya Sakata*

Cite This: *ACS Omega* 2024, 9, 49368−49376

Read Online

ACCESS | Metrics & More | Article Recommendations | Supporting Information

ABSTRACT: In this study, we realized a real-time and enzyme-free measurement of lactate in sweat in the same way as an enzyme-based amperometric method. A conductive polymer, which is based on polyaniline (PANI), was strongly coated on a glassy carbon electrode as a poly *m*-aminophenylboronic acid (PANI−PBA) membrane by drop-casting, which is a convenient method, owing to adhesive phytic acid (PA) molecules with negative charges included as a dopant. This polymer membrane had a functional structure with PBA in the PANI main chain, which expectedly induced electrical charges upon diol binding to lactate, owing to the formation of deprotonated boronate esters with negative charges. This indicates that PBA served as the self-dopant and as the site of binding to lactate. On the basis of the fundamental electrochemical characteristics such as the membrane resistance, the change in the current density of the PA-doped PANI−PBA electrode was quantitatively monitored with the change in lactate concentration from 1 to 300 mM under acidic conditions in real time, considering pH and interfering substances in sweat. Moreover, the sweat lactate concentration was determined to be ca. 60 mM using the PA-doped PANI−PBA electrode in a microfluidic system in measurements using sweat samples collected during exercise load. A change in current density induced a change in the density of charges in the capacitive PA-doped PANI−PBA membrane. This means that the detection mechanism for the change in the lactate concentration in sweat was based on repeated charging and discharging in the PA-doped PANI−PBA electrode.

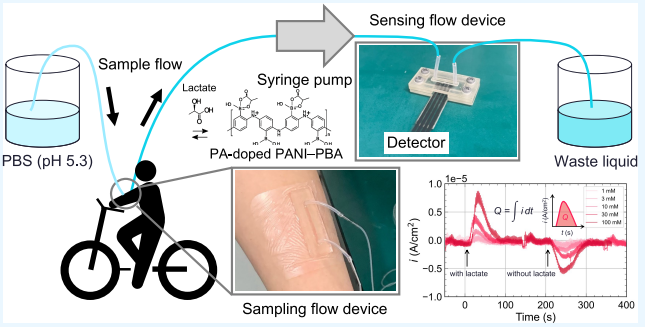

1. INTRODUCTION

Lactate is used as a biomarker for the early diagnosis of, for example, pressure ischemia and cystic fibrosis under hypoxic conditions,[1,2] which contributes to the prevention of ischemic pressure ulcers. As the amount of oxygen in muscle cells decreases during anaerobic exercise, the energy metabolism switches from the citric acid cycle to the glycolysis system, which results in the production of lactate. Considering this metabolic mechanism, the relationship between lactate concentration and exercise load has been widely examined in various studies, the results of which suggest that lactate is a useful biomarker for evaluating exercise load.[3−5] In other words, the blood lactate concentration is recognized as an indicator of training intensity and is considered important for the control of athletic performance in sports medicine.[6]

However, it is invasive to collect blood samples and difficult to continuously monitor the lactate concentration in the blood during exercise. On the other hand, lactate concentration is relatively high in sweat; that is, it is approximately 4−25 mM in the sweat of a healthy person and further increases to 50−80 mM during an exercise load.[7] In addition, the sweat lactate concentration is known to show a strong correlation with the blood lactate concentration;[8] therefore, it is an attractive indicator for the noninvasive and real-time measurement of sweat lactate concentration during an exercise load.

A conventional lactate biosensor is based on an amperometric measurement of hydrogen peroxide generated by an enzymatic reaction.[9−11] Enzymes contribute to the desired specificity to and selectivity for target biomolecules detected as expected; however, they have problematic issues, namely, their relatively short shelf lives and high costs, because they are biological raw materials and applicable to only limited types of biomarker. Therefore, a versatile platform composed of artificial functional membranes is required and proposed for enzyme-free biosensors.

Among such artificial functional membranes, conductive polymers are promising membrane materials to functionalize and induce electrical signals to detect target biomarkers such as lactate.[12,13] Polyaniline (PANI) is an artificial conductive

Received: July 18, 2024
Revised: October 23, 2024
Accepted: December 3, 2024
Published: December 9, 2024

Scheme 1. Schematic of Polymerization of *m*-Amino−PBA to PANI−PBA (Top) and Diol-Based Reversible Binding of Lactate and PBA (Bottom)

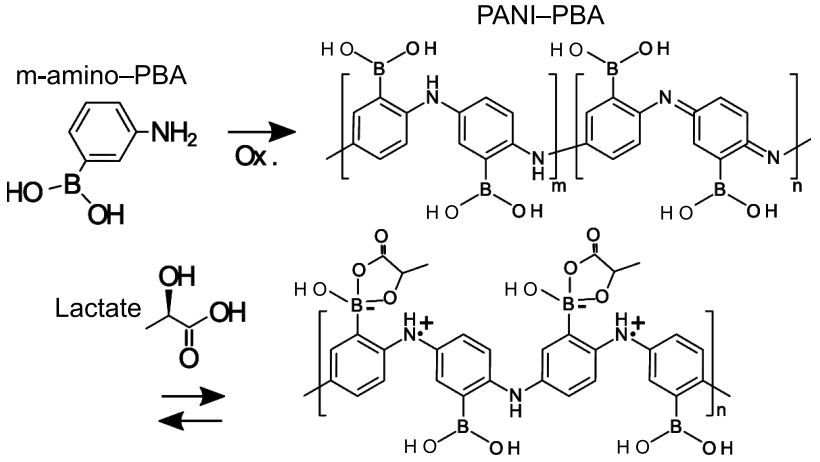

polymer that has a longer shelf life, is more cost-effective than enzymes, and can be easily functionalized by adding functional groups. PANI shows the transitions among the pernigraniline, emeraldine, and leucoemeraldine base forms on the basis of the redox reactions.[14,15] In particular, the protonated emeraldine base PANI (emeraldine salt), which is often obtained by electropolymerization under acidic conditions, shows high conductivity. This is why, the addition of dopants with negative charges induces the protonation of PANI and results in a superior conductivity even under neutral conditions.[15] Also, the polymerization of *m*-aminophenylboronic acid (*m*-amino−PBA) to obtain PANI−PBA hardly proceeds because the meta-substituted, strong electron-withdrawing boronic acid moiety inhibits the electrophilic attack by the radical cations.[16] Therefore, fluoride ions that strongly bind boronic acids, thereby altering the electron affinity, are often utilized for successful polymerization.[17] Recently, a phytic acid (PA)-doped PANI system has been proposed for its simplicity and versatility, instead of fluoride ions.[18−20] PA is a natural product that is abundant in plants. The capability of PA to adhere to various surfaces enables the versatile functionalization of different electrode surfaces.[21] Simultaneously, the electrostatic interaction between negatively charged PA and *m*-amino−PBA affects the electron affinity of the monomer and facilitates the polymerization to PANI−PBA. Moreover, PANI−PBA has the functional structure with PBAs in the PANI main chain, which expectedly induces electrical charges upon diol binding to some biomolecules such as lactate owing to the formation of deprotonated boronate esters with negative charges (Scheme 1).[12,13,20] That is, such boronic acid groups play the role of self-doping in PANI after their reaction with lactate, which results in an increase in PANI conductivity. Fortunately, the binding constant between PBA and lactate ($K_a^{PBA\text{-}lac}$) is higher under more acidic conditions ($pK_a^{PBA\text{-}lac} \approx 3.7$),[22] that is, a PA-doped PANI−PBA is expected to show a change in conductivity on the basis of PBA−lactate complexes in sweat samples (pHs 5−6),[23] which is easily immobilized on electrode surfaces.

Considering the above, we can expect a change in the resistance of PANI−PBA on the basis of the PBA−lactate interaction, as reported previously.[13] However, this finding was based on impedance spectra, which were not measured in real time for the change in the lactate concentration. Moreover, PANI-based membranes were mostly coated on electrode surfaces by electropolymerization,[13,24−26] in which electron donors such as fluoride ions were included, taking advantage of the conductivity of the membranes; however, the coating process is slightly tedious. In this study, we employed PA as the dopant in PANI−PBA, which results in the electrostatic interaction between PANI−PBA and a carbon electrode as well in a fluoride-free manner; thus, the PA-doped PANI−PBA membrane can be easily coated on the electrode surface by drop-casting. Using the PA-doped PANI−PBA electrode, we examined its fundamental electrical characteristics, such as membrane resistance, by cyclic voltammetry (CV) and electrochemical impedance spectroscopy (EIS) to determine the change in the concentration of not only lactate but also sodium chloride (NaCl) and glucose, which are the main components in sweat. On the basis of the fundamental electrical characteristics, the change in the current of the PA-doped PANI−PBA electrode was monitored as the indicator of the change in lactate concentrations at a constant bias voltage in real time, and then the detection mechanism was examined as a topic in this paper. Eventually, the sweat lactate concentration was continuously monitored using a microfluidic system with the PA-doped PANI−PBA electrode in which a sweat sample was collected by flowing a buffer solution. This means that the enzyme-free electrode enables the real-time monitoring of lactate in the same way as the conventional enzyme-based methods.[11,27]

2. EXPERIMENTAL PROCEDURE

2.1. Materials and Chemicals. Chemicals were used as received, unless otherwise stated. *m*-Amino−PBA (85%), aniline (ANI), PA (50% solution in water), ammonium peroxodisulfate (APS, 99%), sodium lactate, glucose, NaCl, hydrochloric acid (HCl), sodium hydroxide (NaOH), sodium perchlorate ($NaClO_4$), nitric acid (HNO_3), sodium dihydrogen phosphate (NaH_2PO_4), disodium hydrogen phosphate (Na_2HPO_4), potassium chloride (KCl), 3.3 M KCl solution containing AgCl, agar (guaranteed reagent), acetone, and methanol were purchased from FUJIFILM Wako Pure Chemical Corporation.

2.2. Coating of PA-Doped PANI−PBA Membrane by Drop-Casting. A rod-type glassy carbon electrode (3 mm diameter, 0.0707 cm^2, ALS Co.) was polished with an alumina

https://doi.org/10.1021/acsomega.4c06671
ACS Omega 2024, 9, 49368−49376

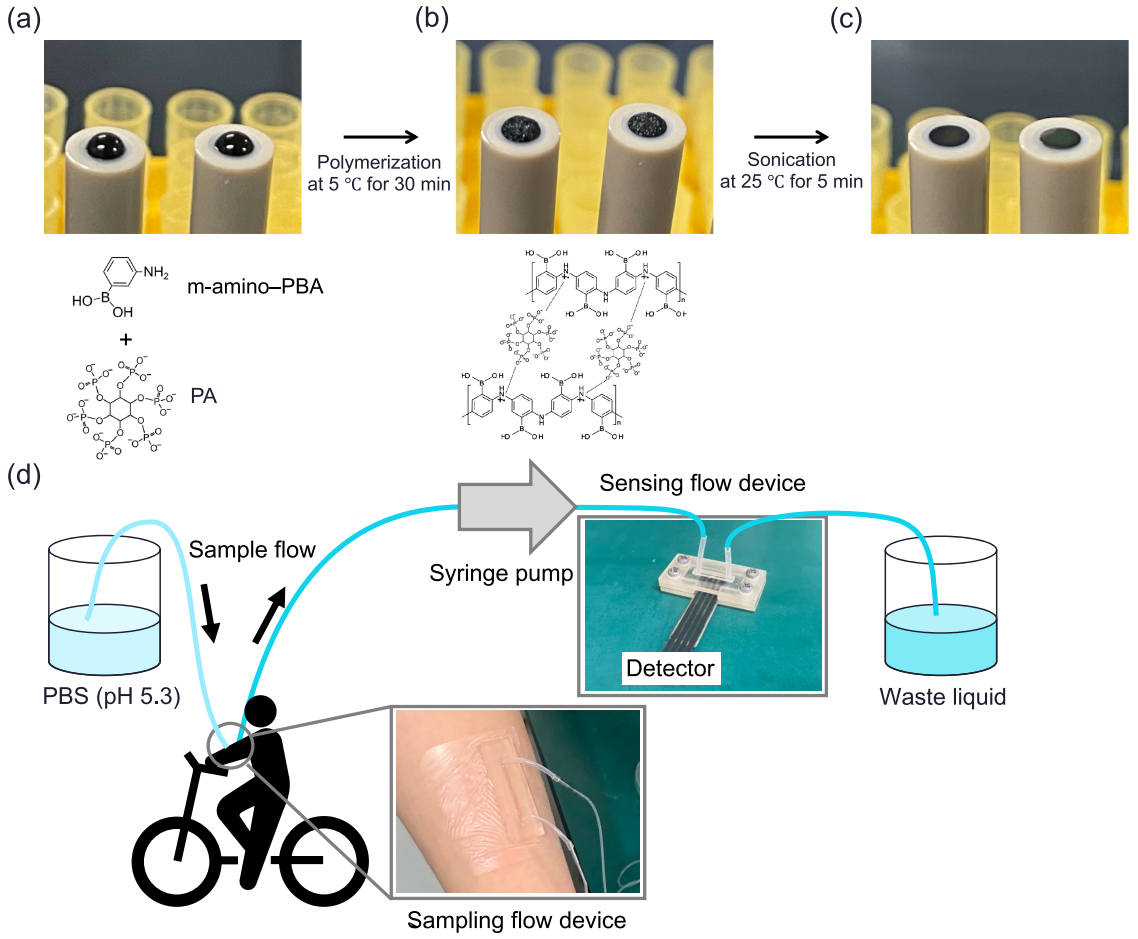

Figure 1. (a) Drop-casting. (b) Polymerization at 5 °C for 30 min. (c) Ultrasonic cleaning at 25 °C for 5 min. A rod-type electrode (glassy carbon) was used in (a–c). (d) Scheme of sweat lactate sensing. The microfluidic system was composed of two devices: the sensing device with the printed sheet electrode (carbon paste) coated with the PA-doped PANI–PBA membrane (Figures S1 and S2) and the sampling device (Figure S3).

slurry (0.05 μm diameter, ALS Co., Ltd.) and sonicated in deionized water (UL-Pure, Komatsu Electronics Co., Ltd.) for 4 min. Then, 40.8 mg of *m*-amino–PBA (or 28.0 mg of ANI) and 40.1 μL of PA were dissolved in deionized water (105.9 μL) to a final volume of 146 μL. Then, another 100 μL of 28.6 mg of APS in the deionized water was prepared. The tubes were kept in an ice bath to keep the temperature below 5 °C. Solutions of *m*-amino–PBA (or ANI) with PA and APS were mixed at a 2/1 v/v ratio and vortexed for 10 s. 5 μL of a mixture was dropped on the electrode (drop-casting) and kept in a refrigerator (5 °C) for 30 min to polymerize (Figure 1a,b). Then, the nonadsorbed components of the membrane were removed by ultrasonic cleaning (Figure 1c). Thus, the PA-doped PANI–PBA or PA-doped PANI membrane was coated on a rod-type glassy carbon electrode. Moreover, the PA-doped PANI–PBA membrane was similarly coated on the electrode sheet mentioned in Section 2.5 by drop-casting. For the PA-doped PANI membrane (control sample without PBA), ANI was used as a monomer instead of *m*-amino–PBA. For comparison, solutions of *m*-amino–PBA with PA and APS and deionized water were mixed at a 1/1/1 v/v/v ratio to decrease the concentrations of *m*-amino–PBA and PA by half (half-concentration PA-doped PANI–PBA). This membrane was coated on a glassy carbon electrode as described above.

2.3. Electrochemical Characterization of PA-Doped PANI–PBA and PANI Membranes. Electrochemical characteristics were measured using a standard electrochemical analyzer (618E, ALS Co., Ltd.) with a three-electrode setup. A platinum wire electrode (0.78 cm^2) and a laboratory-produced Ag/AgCl electrode were used as the counter and reference electrodes, respectively. The reference electrode was inserted into the analyte solution through a salt bridge filled with an agarose gel containing 3.3 M KCl. The inner solution of the reference electrode was 3.3 M KCl containing AgCl, into which the Ag/AgCl electrode was inserted. As the measurement solutions, a 100 mM phosphate buffer was first prepared by mixing 5.873 g of NaH_2PO_4 and 0.220 g of Na_2HPO_4 in about 400 mL of deionized water, and pH was adjusted to 5.3 by adding HCl or NaOH. Then, $NaClO_4$ or NaCl was added at a concentration of 300 mM in the 100 mM phosphate buffer, the pH of which was controlled to 5.3 by adding HCl or NaOH. Another 100 mM phosphate buffer was prepared with 300 mM sodium lactate instead of $NaClO_4$ or NaCl (pH 5.3). In the electrochemical measurements of lactate, the measurement solutions were maintained at a constant ionic strength by exchanging a certain amount of 100 mM phosphate buffer, including 300 mM $NaClO_4$ with a certain amount of 100 mM phosphate buffer, including 300 mM sodium lactate or 300 mM NaCl. This resulted in a change in lactate concentration at the constant ionic strength and pH of measurement solutions. In other words, the solution resistance (R_s) was maintained to be constant.

The PA-doped PANI–PBA membrane was characterized by CV in 100 mM phosphate buffer with 300 mM $NaClO_4$ for

https://doi.org/10.1021/acsomega.4c06671
ACS Omega 2024, 9, 49368–49376

five cycles. Potential was applied between −0.20 and 0.55 V at a scan rate of 100 mV/s. EIS was carried out using the same electrochemical setup described above. First, the impedance spectra of the PA-doped PANI−PBA and PANI-modified electrode systems were collected in the above-mentioned phosphate buffer (pH 5.3) by changing the concentrations of lactate, NaCl, and glucose (c) within 0, 1, 3.16, 10, 31.6, and 100 mM. An open circuit potential (OCP) of 0.11 V was applied as the initial potential in this study, which may be near the half-wave potential ($E_{1/2}$). The frequency was varied from 100 kHz to 0.1 Hz.

2.4. Surface Characterization of PA-Doped PANI−PBA and PANI Membranes. The surface morphologies and thicknesses of the PA-doped PANI−PBA and PANI membranes were determined by AFM (Nanoscope IIIa, Veeco Instruments Inc.). A glass substrate was coated with the PA-doped PANI−PBA and PANI membranes, as described above. The glass substrate was sonicated in acetone, methanol, and deionized water, each for 5 min, before the functionalization. The thickness of the PA-doped PANI−PBA and PANI membranes was measured at a step of their membranes against the substrate surface, which was formed by covering the substrate with a poly(dimethylsiloxane) (PDMS, SYLGARD 184 Silicone Elastomer Kit, Dow Corning) sheet during polymerization, after which it was peeled off.

2.5. Real-Time Measurement of Sweat Lactate with Microfluidic System. The microfluidic system was prepared according to the fabrication process described in a previous paper.[11] Instead of the enzyme-based lactate biosensor, the PA-doped PANI−PBA lactate biosensor was used in the microfluidic system in this study. This system was composed of two devices: sensing and sampling devices (Figure 1d).

To combine the PA-doped PANI−PBA electrode in the sensing device, the working, reference, and counter electrodes were prepared by conventional screen printing (Figure S1). A carbon graphite paste (C2070424D2, Sun Chemical) was printed on a poly(ethylene terephthalate) (PET) sheet (100 μm) and then dried at 90 °C for 20 min. Two electrodes were coated with the PA-doped PANI−PBA membrane to form the working electrode (drop-casting). A silver−silver chloride paste (BAS Inc.) was printed on one of the electrodes to form the reference electrode. The remaining carbon electrode was used as the counter electrode. In the fabrication of the sensing device, a channel mold (length: 15 mm, width: 1 mm, depth: 1 mm) and three parts of the sensor case were formed on the poly(methyl methacrylate) (PMMA) substrate using a 3D printer (AGILISTA-3200, Keyence); then, PDMS was poured into the channel mold to form the flow channel. The flow channel was attached to the PA-doped PANI−PBA electrode sheet, which was packaged in three case parts (Figure S2).

Similarly, we fabricated the sampling device composed of PDMS (length: 30 mm, width: 2 mm, depth: 1 mm), which was directly fixed on the arm's skin surface using a medical adhesive plaster (NIPRO), as shown in Figure S3. Then, even in the case of low perspiration, lactate secreted from sweat glands can be collected by streaming the measurement solution as a carrier in the flow channel. The measurement solution that passed through the sampling device and included lactate was fed to the sensing device via a microtube and measured by the PA-doped PANI−PBA electrode (Figure 1d).

In the electrochemical measurement with the microfluidic system, we employed the real-time measurement of current at a constant bias voltage of 0.11 V (initial potential), although the fundamental CV curves were measured to confirm the conductivity of the PA-doped PANI−PBA electrode before the real-time measurement. First, the same measurement solution described in Section 2.2 was used to maintain the ionic strength and pH when the change in current was monitored with the changes in lactate and NaCl concentrations (0, 1, 3.16, 10, 31.6, 100, and 300 mM) in the sensing device but without the sampling device; the suction rate of the syringe pump was set to 300 μL/min. Next, in the sweat lactate measurement, 100 mM phosphate buffer (pH 5.3) was allowed to flow in the microfluidic system for collecting and detecting sweat samples (Figure 1d). A healthy adult male wearing the system warmed up sufficiently, performed exercises on a stationary bike for about 15 min, then rested for about 15 min, and the change in lactate concentration was examined. At the same time, the amount of sweat produced was measured using a microperspiration meter (TPL3520, Techno Science Co., Japan). All experiments were conducted indoors at a temperature of 23 °C and a humidity of 40−50%; the suction rate of the syringe pump was set to 5 μL/min.

3. RESULTS AND DISCUSSION

3.1. Fundamental Characteristics of PA-Doped PANI−PBA Membrane Coated on Rod-Type Electrode by Drop-Casting. The PA-doped PANI−PBA membrane was coated on a glassy carbon electrode by drop-casting (Figure 1a−c). The drop-casting technique is a facile and versatile fabrication process to functionalize surfaces of various substrates, that is, not only conductive electrodes but also insulators such as oxides, although an electropolymerization method is basically limited to conductive electrodes. Furthermore, the fabricated membrane was sticky on the electrode surface owing to adhesive PA molecules included in it.[21] As shown in Figure S4a, the thickness of the PA-doped PANI−PBA membrane obtained in this study was approximately 100 nm, which was measured by AFM. In addition, the thickness was decreased to half, approximately 50 nm, by reducing the concentrations of the components *m*-amino−PBA and PA during polymerization by half, while maintaining the concentration ratio of each component (i.e., half-concentration PA-doped PANI−PBA). Therefore, the thickness of the PA-doped PANI−PBA membrane is easily controlled by varying the concentrations of components for drop-casting polymerization. Moreover, as shown in Figure S4b, the CV curve of the PA-doped PANI−PBA electrode in the buffer solution (pH 5.3) was obtained, showing the oxidation−reduction reaction, the trend of which was found to be similar to that of a polymeric PANI−PBA membrane.[20] $E_{1/2}$ was estimated to be around 0.11 V, which was near the OCP of the PA-doped PANI−PBA (emeraldine salt). Then, the Nyquist plot prepared using the results of the EIS measurement is shown in Figure S4c. On the basis of an equivalent circuit of a conductive polymer membrane (see inset in Figure S4c), the membrane resistance (R_m) and Warburg impedance (Z_W) in series and the membrane capacitance (C_m) constitute the circuit in parallel, although some other circuits of PANI membranes were proposed in previous works.[13,28−30] The data plots were fitted well in accordance with this circuit model, and then, the $R_m^{PANI-PBA}$ of the PA-doped PANI−PBA membrane was calculated as the diameter of the semicircle in the Nyquist plot along the real axis of the impedance Z (Z'). When a constant-phase element (CPE) is added to the equivalent circuit considering the surface roughness and other properties

https://doi.org/10.1021/acsomega.4c06671
ACS Omega 2024, 9, 49368−49376

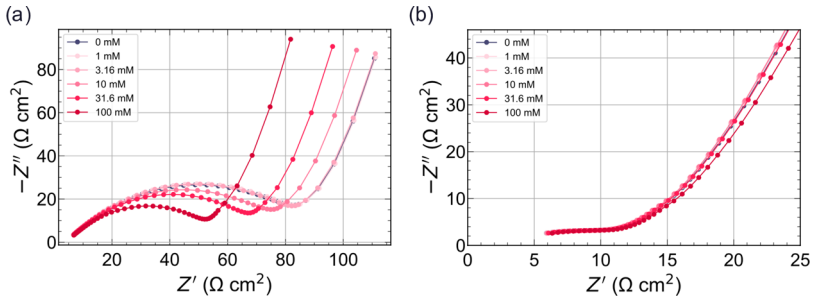

Figure 2. Nyquist plot for changes in lactate concentrations (1−100 mM) measured with PA-doped PANI−PBA (a) and PA-doped PANI (b) coated on a rod-type glassy carbon electrode. The measurements were performed in 100 mM phosphate buffer with 300 mM $NaClO_4$ (pH 5.3) to maintain the ionic strength of Na^+ even when a certain volume of a lactate solution was exchanged with the buffer at each lactate concentration. This is why, the solution resistance (R_s) remained constant. The frequency was varied from 100 kHz to 0.1 Hz.

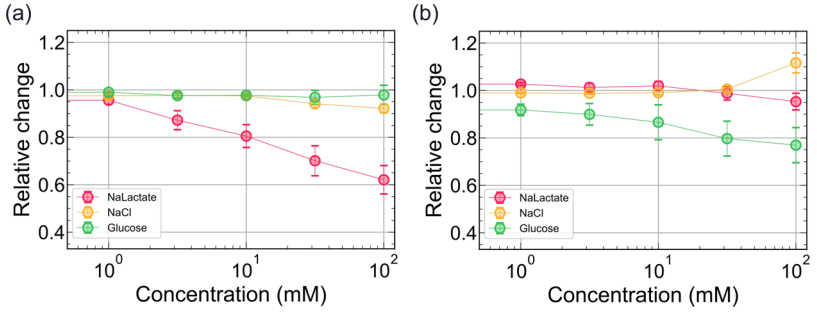

Figure 3. Relative changes in membrane resistance (R_m) with changes in lactate, NaCl, and glucose concentrations (1−100 mM) measured with a PA-doped PANI−PBA electrode at pH 5.3 (a) and 7.4 (b). The error bars represent the standard error (n = 4).

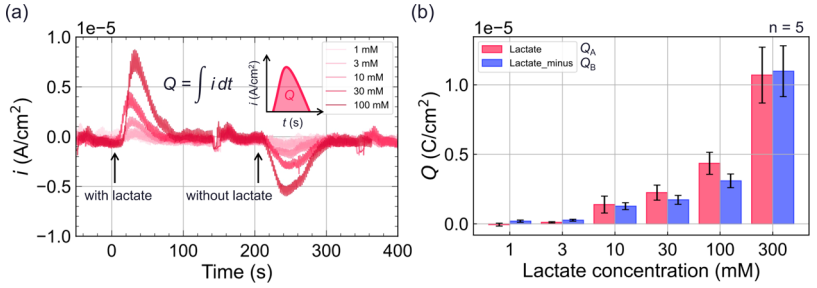

Figure 4. (a) Change in current density (i) with change in lactate concentration (1−100 mM) measured with printed sheet electrode (carbon paste) coated with PA-doped PANI−PBA membrane in a microfluidic system. The buffer solution with or without lactate was allowed to flow within 0−200 or 200−400 s, respectively. (b) Change in charge (Q) with change in lactate concentration (1−300 mM). Q was calculated by the integration of the change in i with the reaction time on the basis of the data shown in (a). The error bars represent the standard error (n = 5).

of the PA-doped PANI−PBA membrane (Figure S4d),[31,32] the modified circuit may be fitted with the data relatively well, although the details should be examined in the future. Moreover, $R_m^{PANI-PBA}$ was compared to the membrane resistance of the PA-doped PANI without PBA (R_m^{PANI}) in the measurement of the change in lactate concentration. When the lactate concentration was increased, $R_m^{PANI-PBA}$ decreased, whereas R_m^{PANI} hardly changed, as shown in Figure 2. This indicates that the decrease in $R_m^{PANI-PBA}$ was due to the increase in the density of deprotonated boronic acid−lactate complexes with negative charges; that is, such negatively charged complexes worked as the dopants in the PA-doped PANI−PBA membrane. Furthermore, the fundamental electrical characteristics of the PA-doped PANI−PBA electrode should be examined in relation to the changes in not only the concentration of lactate but also those of other components such as NaCl and glucose, considering the measurement of sweat lactate in real time. Figure 3 shows the relative changes in $R_m^{PANI-PBA}$ (Δr) with changes in the concentrations of lactate, NaCl, and glucose. Δr is defined as

$$\Delta r = 1 - \frac{R_m^{PANI-PBA}(c)}{R_m^{PANI-PBA}(0)} \quad (1)$$

where $R_m^{PANI-PBA}(c)$ and $R_m^{PANI-PBA}(0)$ are the membrane resistances at c mM and 0 mM for lactate, NaCl, and glucose, respectively. As shown in Figure 3a based on the data obtained in Figure 2a, at pH 5.3, the Δr of lactate clearly decreased with an increasing lactate concentration. On the other hand, $R_m^{PANI-PBA}$ hardly changed upon adding NaCl or glucose. In particular, glucose appeared not to affect the conductivity of the PA-doped PANI−PBA membrane at pH 5.3. In contrast, at pH 7.4, the Δr of glucose decreased with an increasing glucose concentration, whereas those of lactate and NaCl were significantly small (Figure 3b). Thus, the PA-doped PANI−PBA membrane may show selectivity for lactate or glucose,

https://doi.org/10.1021/acsomega.4c06671
ACS Omega 2024, 9, 49368−49376

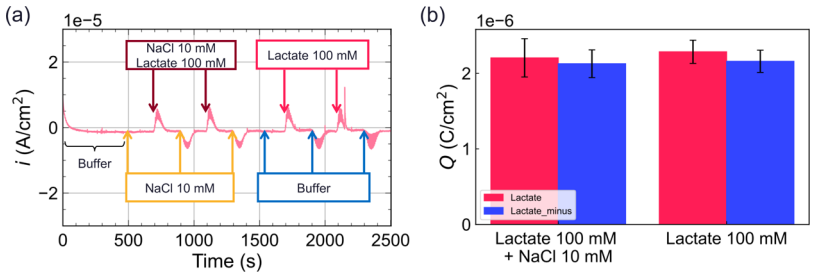

Figure 5. (a) Change in current density (i) upon adding 10 mM NaCl, 100 mM lactate, the mixture, or buffer without NaCl and lactate at pH 5.3 measured with printed sheet electrode (carbon paste) coated with PA-doped PANI−PBA membrane in a microfluidic system. The measurement solutions were suctioned and allowed to flow at a rate of 300 μL/min through the sensing device. (b) Change in charge (Q) upon adding 100 mM lactate or a mixture of 10 mM NaCl and 100 mM lactate. Q was calculated by the integration of the change in i with reaction time on the basis of the data shown in (a). The error bars represent the standard error (n = 4).

depending on pH. Most boronate esters as well as the PBA−glucose ester show relatively higher binding constants in neutral to alkaline solutions.[33,34] This is why the selective detection of lactate is expected in acidic sweat, using the PA-doped PANI−PBA membrane for which the binding constant of the PBA−lactate ester should be relatively high; however, it should be examined whether diol compounds as interfering species against lactate are abundant in sweat.

3.2. Real-Time Monitoring of Lactate Concentration Using PA-Doped PANI−PBA Coated on Printed Film Electrode by Drop-Casting. Considering the trend of $R_m^{PANI-PBA}$ in relation to the change in lactate concentration, we can simply measure the change in the current of the PA-doped PANI−PBA electrode at a constant bias voltage upon adding lactate in real time. In this case, a microfluidic system with the printed electrodes coated with the PA-doped PANI−PBA membrane (ca. 100 nm thickness) was utilized to continuously flow the buffer solutions with or without lactate. As shown in Figure 4, the current density increased upon adding lactate and subsequently gradually decreased to the initial level within the range of 0−200 s, whereas it oppositely decreased upon adding the same buffer without lactate within the range of 200−400 s. This is consistent with the reversible reaction between PBA and lactate under acidic condition. In addition, the amount of change in current density increased with lactate concentration from 1 to 100 mM. It is considered that this signal trend was derived from the storage of charges generated by the PBA−lactate complexes per surface area (Q), which was calculated by integrating the change in current density with the change in time (*see* inset in Figure 4a). On the other hand, the opposite signal trend may have been caused by the dissociation of such complexes to noncharged PBA. Indeed, as shown in Figure 4b, Q increased with lactate concentration ($+\Delta Q_A$), whereas it decreased by almost the same amount as ΔQ_A ($-\Delta Q_B$) after adding the same buffer without lactate, depending on the lactate concentration. By analyzing the changes in parameters over time, we observed that first, $R_m^{PANI-PBA}$ decreases from $R_m^{PANI-PBA}(0)$ ($-\Delta R_m^{PANI-PBA}$) at the initial potential of 0.11 V ($V(0)$) accompanied by the formation of negatively charged PBA−lactate esters. Then, $-\Delta R_m^{PANI-PBA}$ contributes to the increase in current density ($+\Delta I$) from the initial current density ($I(0) \approx 0$), which induces the storage of charges ($+\Delta Q_1$). At the equilibrium state of PBA−lactate complexes (i.e., $R_m^{PANI-PBA}(0) - \Delta R_m^{PANI-PBA}$), the current density $I(0) + \Delta I$ gradually decreases to $I(0)$ at a constant $V(0)$ while charge storage proceeds in accordance with the decrease in current density ($+\Delta Q_2$), which results in $+\Delta Q_A = +\Delta Q_1 + \Delta Q_2$, retaining the concentration of negatively charged PBA−lactate esters. On the other hand, in accordance with the dissociation of negatively charged PBA−lactate esters upon adding the buffer without lactate, $R_m^{PANI-PBA}$ returns to the initial $R_m^{PANI-PBA}(0)$ ($+\Delta R_m^{PANI-PBA}$), and simultaneously the stored charge ΔQ_A is discharged ($-\Delta Q_1$), which provides $-\Delta I$. Subsequently, $-\Delta Q_2$ is discharged accompanied by $-\Delta I$ at $R_m^{PANI-PBA}(0)$ and a constant $V(0)$. Eventually, the current density returns to its initial value, which means that the PA-doped PANI−PBA is reusable for monitoring lactate concentration in samples, such as sweat. That is, the current flow was associated with the equilibrium state of PBA−lactate complexes, although the charging and discharging may have changed the redox potential of PANI−PBA under a constant voltage of 0.11 V.[35] Thus, the detection principle of lactate in the amperometric real-time measurement was based on repeated charging and discharging in the PA-doped PANI−PBA electrode, corresponding to the reversible reaction of PBA with lactate. On the basis of this detection principle, the PA-doped PANI−PBA electrode may enable the simple and real-time measurement of various biomolecules such as glucose and dopamine as well as lactate, depending on pH. Moreover, the concentration of NaCl in sweat is approximately 30−80 mM,[36,37] which is almost the same as that of lactate, which is significant for one of the interfering species. On the other hand, the concentration of glucose in sweat is sufficiently lower than those of lactate and NaCl (ca. 0.1 mM),[13] which is negligible. Indeed, the characteristic signals strongly depended on the lactate concentration, regardless of the presence of NaCl in the measurement solutions (Figure 5a,b). Also, this can be supported by the data shown in Figure 3, where NaCl hardly contributed to the change in $R_m^{PANI-PBA}$ with the change in the concentration of NaCl from 1 to 100 mM. Thus, the change in the lactate concentration can be simply and continuously monitored from the change in the current density of the PA-doped PANI−PBA electrode in the microfluidic system, even when NaCl is present in large amounts in samples, such as sweat.

In the PA-doped PANI−PBA membrane, PBA is the binding site of lactate, which is based on a one-to-one reversible reaction. That is, the adsorption of lactate on and/or in the PA-doped PANI−PBA membrane can be analyzed on the basis of the Langmuir adsorption isotherm. In particular, ΔQ is based on the change in the density of molecular charges of boronate esters with lactate in equilibrium. Therefore, ΔQ can

https://doi.org/10.1021/acsomega.4c06671
ACS Omega 2024, 9, 49368−49376

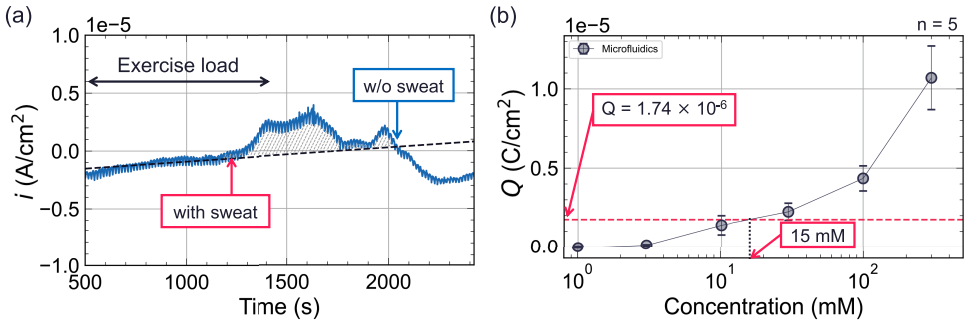

Figure 6. (a) Change in current density (i) during exercise load measured with printed sheet electrode (carbon paste) coated with PA-doped PANI−PBA membrane in the microfluidic system. The pH 5.3 buffer solution was suctioned and allowed to flow at a rate of 5 μL/min through the sampling and sensing devices. (b) Change in charge (Q) with a logarithmic change in lactate concentration (1−300 mM), which was based on Figure 4b. Q estimated in (a), which was derived from sweat lactate, is indicated by a dotted line. The concentration of sweat lactate diluted in the microfluidic system was estimated to be approximately 15 mM. The error bars represent the standard error (n = 5).

be expressed with the Langmuir adsorption isotherm equation as

$$\Delta Q = \frac{\Delta Q_{max} K_a C}{1 + K_a C} \quad (2)$$

Here, ΔQ_{max} is the maximum amount of change in stored charges attributable to the change in current density based on the formation of boronate esters with lactate in the PA-doped PANI−PBA membrane with a constant thickness, which is proportional to the density of binding sites. K_a is the binding constant based on the interaction between PBA and lactate. The data shown in Figure 4b were fitted with eq 2; as a result, K_a was calculated as approximately 13.1 M^{-1} (pH 5.3). This value was in good agreement with K_a for the nonimprinted PANI−PBA reported in a previous paper.[13] In other words, the imprinting of lactate in the PA-doped PANI−PBA membrane may enhance some sensing performance characteristics such as the LOD as well as K_a in the real-time measurement of current density.

3.3. Sweat Lactate Monitoring Using Microfluidic System with PA-Doped PANI−PBA Electrode. Considering the above concept, the lactate concentration was continuously monitored while sweat samples were collected during an exercise load, as shown in Figure 6. The pH 5.3 buffer solution was suctioned and allowed to flow at a rate of 5 μL/min through the sampling device, which was attached to the upper arm, and the sensing device in this order by using a syringe pump (Figure 1d). Then, we collected sweat from the skin surface into the sampling device (ca. 2 mg/cm^2/min) and then output the change in the current density of the PA-doped PANI−PBA electrode to measure the sweat sample in the sensing device, as shown in Figure 6a. The exercise was continuously performed within 0−900 s. After the exercise load, the collected sweat sample had reached the sensing device, and then the current density gradually increased, which indicates charging of the PA-doped PANI−PBA, although it took some time for the sample to reach the sensing device because of the distance between the sampling and sensing devices. Moreover, the signals fluctuated slightly, because it took a while for the collected sweat to uniformly mix with the buffer. In accordance with the calculation mentioned in the above section, Q was calculated to be 1.74 × 10^{-6} C/cm^2 (shaded area). Considering the calibration curve of Q for the change in log c shown in Figure 6b, which was based on Figure 4b, the measured solution was found to include lactate with a concentration of approximately 15 mM. The lactate concentration in sweat is approximately 80 mM at most.[7] Considering the flow rate (5 μL/min), the amount of sweat (ca. 2 mg/cm^2/min), and the surface area of the sampling device (3 × 0.2 cm^2), we considered that the collected sweat was diluted about 4-fold in the buffer, that is, the concentration of lactate actually detected was approximately 60 mM in this measurement (exercise load). Considering the data shown in a previous paper,[11] this lactate concentration would have been based on lactate secretion during an anaerobic exercise. Moreover, we also confirmed that the current density decreased as sweating subsided and sweat disappeared in the flowing buffer, which indicates discharging of the PA-doped PANI−PBA. Thus, not only can sweat samples be collected with the microfluidic system and quantified at diluted amounts but also the enzyme-free and real-time detection of lactate in sweat is realized with the PA-doped PANI−PBA electrode, which detects the change in current density on the basis of the formation of negatively charged boronate esters with lactate. This study demonstrated that the system we developed is useful for enzyme-free and simple amperometric real-time monitoring of lactate in human sweat. However, perspiration is affected by several factors such as the mental condition and body temperature, which are regulated by different mechanisms.[38] Therefore, this system should be applied to the detection of lactate secreted on the basis of various perspiration mechanisms in the future.

As shown in Figures 4 and 5, we needed to repeat the charging and discharging based on the binding and dissociation between lactate and PA-doped PANI−PBA to quantitatively measure the lactate concentration in continuous flow mode. That is, during charging, the current density decreased to zero after increasing owing to the binding between lactate and PA-doped PANI−PBA even when the chemical reaction was maintained in equilibrium. Therefore, discharging based on the dissociation of the lactate/PANI−PBA complex was needed to continuously measure the next lactate concentration by flowing the buffer solution without lactate (Figures 4 and 5). This method may be closer to the flow-injection analysis (FIA), which involves a washing step after sample injections.[39] On the other hand, the buffer solution with and without the sweat sample should have also been flowed and measured alternately on the basis of charging and discharging repeatedly to quantitatively analyze the lactate concentration in the sweat sample. However, there would have been a time lag owing to the charging and discharging to monitor the sweat sample secreted *in situ*. Even if the FIA mode is employed for this

https://doi.org/10.1021/acsomega.4c06671
ACS Omega 2024, 9, 49368−49376

measurement, it may be difficult to solve the problem concerning time lag. This is due to the capacitive property of conducting polymers such as PANI−PBA, which are different from enzyme-entrapped membranes.[11,27] However, the discharging trend could be observed while the buffer solution was flowed (*see* w/o sweat in Figure 6a). This means that the sweat sample was collected and then disappeared as the buffer solution flowed. In particular, *Q*, which was obtained while flowing the buffer solution with the sweat sample, could be estimated to calculate the lactate concentration with some increase or decrease in the current density in this section from the calibration curve shown in Figure 6b. Then, discharging (*see* w/o sweat in Figure 6a) would allow for the subsequent secretion of sweat. In any case, the *in situ* quantitative analysis of lactate in sweat samples without a time lag may be difficult regardless of whether the continuous flow mode or the FIA mode is employed.

4. CONCLUSIONS

The conductive PA-doped PANI−PBA membrane was coated on the glassy carbon electrode simply by drop-casting, the thickness of which was controllable by changing the monomer concentration. PA was included not only as a dopant but also for the enhancement of adhesiveness with the electrode surface. Moreover, PBA preferentially bound to lactate in an acidic solution (e.g., pH 5.3) such as sweat and then induced negative charges as another dopant in the PA-doped PANI−PBA membrane owing to the formation of boronate esters. This is why the PA-doped PANI−PBA electrode showed a decrease in membrane resistance with an increasing lactate concentration in EIS measurements. Moreover, the addition of NaCl and glucose did not generate noise signals for the PA-doped PANI−PBA electrode in the acidic solution, which were assumed as interfering substances in sweat lactate sensing. On the other hand, glucose was preferentially detected in the neutral solution by the PA-doped PANI−PBA electrode, depending on the ionization constant pK_a values of PBA and its esters.

Moreover, the change in the current density of the PA-doped PANI−PBA electrode was monitored with the change in lactate concentration in the acidic solution at a constant bias in real time, considering the change in membrane resistance in the EIS measurement. From the electrical signal waveform, the detection mechanism for the change in lactate concentration was based on repeated charging and discharging in the PA-doped PANI−PBA electrode, corresponding to the reversible reaction of PBA with lactate. This is a very simple detection scheme comparable to that of enzyme electrodes. Moreover, the microfluidic system facilitated sweat collection from the skin surface and the detection of its component with the electrode; that is, a sweat sample was collected with the sampling device, and then the lactate concentration was measured with the PA-doped PANI−PBA electrode in the sensing device. As a result, the concentration of lactate in sweat could be continuously measured during an exercise load and was determined to be approximately 60 mM in that case. Thus, the microfluidic system with the PA-doped PANI−PBA electrode is useful for a stable and reliable continuous measurement of human sweat lactate, and in the future, it will be applied to analyzing and elucidating various perspiration mechanisms in humans.

■ ASSOCIATED CONTENT

Supporting Information

The Supporting Information is available free of charge at https://pubs.acs.org/doi/10.1021/acsomega.4c06671.

Preparation of PA-doped PANI−PBA membrane coated on printed film electrode (Figure S1); preparation of sensing flow device with printed film electrode (Figure S2); preparation of sampling flow device (Figure S3); and fundamental characteristics of PA-doped PANI−PBA membrane (Figure S4) (PDF)

■ AUTHOR INFORMATION

Corresponding Author

Toshiya Sakata − *Department of Materials Engineering, School of Engineering, The University of Tokyo, Bunkyo-ku, Tokyo 113-8656, Japan;* orcid.org/0000-0003-1246-5000; Email: sakata@biofet.t.u-tokyo.ac.jp

Authors

Ryujiro Kishi − *Department of Materials Engineering, School of Engineering, The University of Tokyo, Bunkyo-ku, Tokyo 113-8656, Japan*

Shoichi Nishitani − *Department of Materials Engineering, School of Engineering, The University of Tokyo, Bunkyo-ku, Tokyo 113-8656, Japan;* orcid.org/0000-0001-6355-6952

Hiroyuki Kudo − *Department of Electronics and Bioinformatics, School of Science and Technology, Meiji University, Kawasaki, Kanagawa 214-8571, Japan*

Complete contact information is available at: https://pubs.acs.org/10.1021/acsomega.4c06671

Notes

The authors declare no competing financial interest.

■ ACKNOWLEDGMENTS

This study was partly supported by the Mirai Program of Japan Science and Technology (JST).

■ REFERENCES

(1) Derbyshire, P. J.; Barr, H.; Davis, F.; Higson, S. P. J. Lactate in human sweat: A critical review of research to the present day. *J. Physiol. Sci.* **2012**, *62*, 429−440.

(2) Robergs, R. A.; Ghiasvand, F.; Parker, D. Biochemistry of exercise-induced metabolic acidosis. *Am. J. Physiol. − Regul. Integr. Comp. Physiol.* **2004**, *287*, 502−516.

(3) Buono, M. J.; Lee, N. V. L.; Miller, P. W. The relationship between exercise intensity and the sweat lactate excretion rate. *J. Physiol. Sci.* **2010**, *60*, 103−107.

(4) van Hall, G. Lactate kinetics in human tissues at rest and during exercise. *Acta Physiol.* **2010**, *199*, 499−508.

(5) Adeva-Andany, M.; Lopez-Ojen, M.; Funcasta-Calderon, R.; Ameneiros-Rodriguez, E.; Donapetry-Garcia, C.; Vila-Altesor, M.; Rodriguez-Seijas, J. Comprehensive review on lactate metabolism in human health. *Mitochondrion* **2014**, *17*, 76−100.

(6) Cairns, S. P. Lactic acid and exercise performance: culprit or friend? *Sports Med.* **2006**, *36*, 279−291.

(7) Pribil, M. M.; Laptev, G. U.; Karyakina, E. E.; Karyakin, A. A. Noninvasive hypoxia monitor based on gene-free engineering of lactate oxidase for analysis of undiluted sweat. *Anal. Chem.* **2014**, *86*, 5215−5219.

(8) Karpova, E. V.; Laptev, A. I.; Andreev, E. A.; Karyakina, E. E.; Karyakin, A. A. Relationship Between Sweat and Blood Lactate Levels

During Exhaustive Physical Exercise. *ChemElectroChem* **2020**, *7*, 191−194.
(9) Perdomo, J.; Sundermeier, C.; Hinkers, H.; Morell, O. M.; Seifert, W.; Knoll, M. Containment sensors for the determination of L-lactate and glucose. *Biosens. Bioelectron.* **1999**, *14*, 27−32.
(10) Shimomura, T.; Sumiya, T.; Ono, M.; Ito, T.; Hanaoka, T. Amperometric L-lactate biosensor based on screen-printed carbon electrode containing cobalt phthalocyanine, coated with lactate oxidase-mesoporous silica conjugate layer. *Anal. Chim. Acta* **2012**, *714*, 114−120.
(11) Enomoto, K.; Shimizu, R.; Kudo, H. Real-time skin lactic acid monitoring system for assessment of training intensity. *Electron. Commun. Jpn.* **2018**, *101*, 41−46.
(12) Andreyev, E. A.; Komkova, M. A.; Nikitina, V. N.; Zaryanov, N. V.; Voronin, O. G.; Karyakina, E. E.; Yatsimirsky, A. K.; Karyakin, A. A. Reagentless polyol detection by conductivity increase in the course of self-doping of boronate-substituted polyaniline. *Anal. Chem.* **2014**, *86*, 11690−11695.
(13) Zaryanov, N. V.; Nikitina, V. N.; Karpova, E. V.; Karyakina, E. E.; Karyakin, A. A. Nonenzymatic sensor for lactate detection in human sweat. *Anal. Chem.* **2017**, *89*, 11198−11202.
(14) Kuramoto, N. Fundamentals and Application of Conducting Polymer Polyaniline. *J. Jpn. Soc. Colour Mater.* **2003**, *76*, 352−359.
(15) Tarver, J.; Yoo, J. E.; Dennes, T. J.; Schwartz, J.; Loo, Y. L. Polymer acid doped polyaniline is electrochemically stable beyond pH 9. *Chem. Mater.* **2009**, *21*, 280−286.
(16) Andreev, E. A.; Komkova, M. A.; Nikitina, V. N.; Karyakin, A. A. Reagentless Impedimetric Sensors Based on Aminophenylboronic Acids. *J. Anal. Chem.* **2019**, *74*, 153−179.
(17) Shoji, E.; Freund, M. S. Potentiometric Sensors Based on the Inductive Effect on the pKa of Poly(aniline): A Nonenzymatic Glucose Sensor. *J. Am. Chem. Soc.* **2001**, *123*, 3383−3384.
(18) Pan, L.; Yu, G.; Zhai, D.; Lee, H. R.; Zhao, W.; Liu, N.; Wang, H.; Tee, B. C.-K.; Shi, Y.; Cui, Y.; Bao, Z. Hierarchical nanostructured conducting polymer hydrogel with high electrochemical activity. *Proc. Natl. Acad. Sci. U.S.A.* **2012**, *109*, 9287−9292.
(19) Zhai, D.; Liu, B.; Shi, Y.; Pan, L.; Wang, Y.; Li, W.; Zhang, R.; Yu, G. Highly sensitive glucose sensor based on pt nanoparticle/polyaniline hydrogel heterostructures. *ACS Nano* **2013**, *7*, 3540−3546.
(20) Nishitani, S.; Man, Y.; Noguchi, T.; Sakata, T. Polyaniline-based nanostructure interface for signal-to-noise ratio enhancement in potentiometric enzyme-free biosensors. *Adv. Mater. Interfaces* **2022**, *9*, No. 2201029.
(21) Wang, Y.; Ma, X.; Wen, Y.; Zheng, Y.; Duan, G.; Zhang, Z.; Yang, H. Phytic Acid-Based Layer-by-Layer Assembly for Fabrication of Mesoporous Gold Film and Its Biosensor Application. *J. Electrochem. Soc.* **2010**, *157*, K5.
(22) Martínez-Aguirre, M. A.; Villamil-Ramos, R.; Guerrero-Alvarez, J. A.; Yatsimirsky, A. K. Substituent effects and pH profiles for stability constants of arylboronic acid diol esters. *J. Org. Chem.* **2013**, *78*, 4674−4684.
(23) Curto, V. F.; Fay, C.; Coyle, S.; Byrne, R.; O'Toole, C.; Barry, C.; Hughes, S.; Moyna, N.; Diamond, D.; Benito-Lopez, F. Real-time sweat pH monitoring based on a wearable chemical barcode micro-fluidic platform incorporating ionic liquids. *Sens. Actuators, B* **2012**, *171−172*, 1327−1334.
(24) Badhulika, S.; Tlili, C.; Mulchandani, A. Poly(3-amino-phenylboronic acid)-functionalized carbon nanotubes-based chemiresistive sensors for detection of sugars. *Analyst* **2014**, *139*, 3077−3082.
(25) Nicolas, M.; Fabre, B.; Marchand, G.; Simonet, J. New Boronic-Acid- and Boronate-Substituted Aromatic Compounds as Precursors of Fluoride-Responsive Conjugated Polymer Films. *Eur. J. Org. Chem.* **2000**, *2000*, 1703−1710.
(26) Song, E.; Choi, J.-W. Conducting Polyaniline Nanowire and Its Applications in Chemiresistive Sensing. *Nanomaterials* **2013**, *3*, 498−523.
(27) Konno, S.; Kudo, H. Fundamental Study of a Wristwatch Sweat Lactic Acid Monitor. *Biosensors* **2024**, *14*, 187.
(28) Rubinstein, I.; Sabatani, E.; Rishpon, J. Electrochemical Impedance Analysis of Polyaniline Films on Electrodes. *J. Electrochem. Soc.* **1987**, *134*, 3078.
(29) Albery, W. J.; Chen, Z.; Horrocks, B. R.; Mount, A. R.; Wilson, P. J.; Bloor, D.; Monkman, A. T.; Elliott, C. M. Spectroscopic and electrochemical studies of charge transfer in modified electrodes. *Faraday Discuss. Chem. Soc.* **1989**, *88*, 247−259.
(30) Skinner, N. G.; Hall, E. A. H. The relevance of an equivalent circuit for polyaniline using immittance spectroscopy. *Synth. Met.* **1994**, *63*, 133−145.
(31) Pajkossy, T. Impedance of rough capacitive electrodes. *J. Electroanal. Chem.* **1994**, *364*, 111−125.
(32) Orazem, M. E.; Tribollet, B. *Electrochemical Impedance Spectroscopy*; John Wiley & Sons: Hoboken, NJ, 2008.
(33) Lorand, J. P.; Edwards, J. O. Polyol Complexes and Structure of the Benzeneboronate Ion. *J. Org. Chem.* **1959**, *24*, 769−774.
(34) Springsteen, G.; Wang, B. A detailed examination of boronic acid−diol complexation. *Tetrahedron* **2002**, *58*, 5291−5300.
(35) Shoji, E.; Freund, M. S. Potentiometric Saccharide Detection Based on the pKa Changes of Poly(aniline boronic acid). *J. Am. Chem. Soc.* **2002**, *124*, 12486−12493.
(36) Yokoyama, Y.; Aragaki, M.; Sato, H.; Tsuchiya, M. Determination of sweat constituents by liquid ionization mass spectrometry. *Anal. Chim. Acta* **1991**, *246*, 405−411.
(37) Taylor, R. P.; Polliack, A. A.; Bader, D. L. The analysis of metabolites in human sweat: analytical methods and potential application to investigation of pressure ischaemia of soft tissues. *Ann. Clin. Biochem.* **1994**, *31*, 18−24.
(38) Lipponen, J. A.; Gladwell, V. F.; Kinnunen, H.; Karjalainen, P. A.; Tarvainen, M. P. The correlation of vectorcardio- graphic changes to blood lactate concentration during an exercise test. *Biomed. Signal Process. Control* **2013**, *8*, 491−499.
(39) Zavolskova, M. D.; Nikitina, V. N.; Maksimova, E. D.; Karyakina, E. E.; Karyakin, A. A. Constant Potential Amperometric Flow-Injection Analysis of Ions and Neutral Molecules Transduced by Electroactive (Conductive) Polymers. *Anal. Chem.* **2019**, *91*, 7495−7499.

https://doi.org/10.1021/acsomega.4c06671
ACS Omega 2024, 9, 49368−49376